

# Capillary electrophoresis in aqueous–organic media Ionic strength effects and limitations of the Hubbard–Onsager dielectric friction model

Kimberly I. Roy, Charles A. Lucy\*

Department of Chemistry, University of Alberta, Edmonton, Alberta T6G 2G2, Canada

Received 20 December 2001; received in revised form 11 March 2002; accepted 14 May 2002

## Abstract

The mobilities of three aromatic sulfonates, ranging in charge from  $-1$  to  $-3$ , were investigated by capillary electrophoresis using buffers containing 0 to 75% ethanol or 2-propanol. *Absolute* mobilities were determined by extrapolation of the *effective* mobilities to zero ionic strength according to the Pitts' equation. For all buffers studied, ions of higher charge experienced larger ionic strength effects. The resulting ionic strength-induced selectivity alterations were more dramatic when organic solvents were present in the media. Furthermore, for different organic modifier types and contents, the magnitude of the ionic strength effect was governed to a large extent by the  $1/(\eta\epsilon^{1/2})$  dependence in the electrophoretic effect of the Pitts' equation. Addition of ethanol or 2-propanol to the electrophoretic media resulted in changes in the *absolute* mobilities of the ions. These solvent-induced mobility changes are attributed to dielectric friction. As predicted by the Hubbard–Onsager model, dielectric friction increased with increasing organic content and with increasing analyte charge. As a result, dramatic changes in the relative *absolute* mobilities were observed, such as a reversal in migration order between sulfonates of  $-1$  and  $-3$  charge in 75% 2-propanol. Within the alcohols, the Hubbard–Onsager model was successful at predicting the relative mobility trends upon changing solvent. However, the *relative* trends observed between acetonitrile–water and alcohol–water media were not consistent with the model. This may be explained by the continuum nature of the model, whereby the different ion–solvent interactions characteristic to each solvent class are not taken into account. © 2002 Elsevier Science B.V. All rights reserved.

**Keywords:** Ionic strength; Buffer composition; Dielectric friction; Capillary electrophoresis; Hubbard–Onsager model; Mathematical modelling; Ethanol; Propanol; Alcohols; Sulfonates

## 1. Introduction

It is well known that the addition of organic solvents to the separation media in capillary electrophoresis can result in dramatic selectivity alterations [1,2]. However, these selectivity changes are not

predicted by the Hückel equation, which is the simplest and most common model for mobility. The Hückel equation is:

$$\mu_o = \frac{q}{6\pi\eta r} \quad (1)$$

where  $\mu_o$  is the analyte's *absolute* mobility (independent of electrolyte ionic strength),  $\eta$  is the solvent viscosity, and  $q$  and  $r$  are the analyte's

\*Corresponding author. Tel.: +1-780-492-0315; fax: +1-780-492-8231.

E-mail address: [charles.lucy@ualberta.ca](mailto:charles.lucy@ualberta.ca) (C.A. Lucy).

charge and radius, respectively. Based on this equation, Jouyban-Gharamaleki et al. [3] have formulated a mathematical model to predict electrophoretic mobilities in hydroorganic media. However, according to the Hückel equation, changes in solvent viscosity will lead to changes in the absolute mobilities of the analytes, but not to changes in their relative mobilities. In other words, the Walden products ( $\mu_0\eta$ ; Ref. [4]) should be constant regardless of the solvent composition. Therefore, other models are required in order to explain the changes in selectivity that are observed on going from aqueous to mixed aqueous–organic media.

Solvent-induced selectivity changes result from one or a combination of the following: (i) changes in solvent pH and analyte  $pK_a$ ; (ii) ionic strength effects; and (iii) ion–solvent interactions. These are discussed in detail below. First, the addition of organic solvents to the electrophoretic media can alter selectivity through changes in the solvent pH and analyte  $pK_a$ . This is most easily understood in terms of a solvent-induced change in the analyte charge ( $q$  in Eq. (1)). Several reports in the literature have dealt with this topic. Sarmini and Kenndler [5–9] have investigated the influence of several organic solvents on the acidity constants and mobilities of aromatic acids. Alternatively, a novel mathematical model has been developed by Guillaume et al. [10] that relates electrophoretic mobility to solvent pH and organic solvent content. Furthermore, Barbosa and co-workers [11,12] have developed a model that describes the influence of pH,  $pK_a$ , and activity coefficients on the mobilities of quinolones in acetonitrile–water media. These models are effective at predicting some selectivity changes that are observed on going from aqueous to mixed aqueous–organic media.

Second, solvent-induced selectivity changes can occur through variations in the ionic strength effects with changing organic solvent type and content. It has been shown that the Pitts' equation is successful in describing the ionic strength dependence of mobility in CE [13]. According to this model (see Eq. (3) in the Results and discussion Section), the ionic strength effect is dependent on the solution viscosity and dielectric constant, both of which are solvent-dependent. Indeed, previous studies have demonstrated much more dramatic ionic strength-

induced selectivity changes in methanol–water [14] and acetonitrile–water [15] media than for pure aqueous media.

Third, solute mobility is affected by ion–solvent interactions. These interactions can be modeled in two fundamentally different fashions. The first and oldest picture is the *solvent-berg* model [16]. In this model, the solvent molecules are immediately adjacent to the ion and are rigidly bound to it. This is what is referred to when one talks of the hydration or solvation shell. However, while this model is conceptually easy to grasp, it is difficult to quantify or predict. Further, it is physically unrealistic in that solvation is a dynamic process.

An alternate model of ion–solvent interactions is *dielectric friction*. This model views ion–solvent interactions as a dynamic perturbation of the solvent orientation caused by the ion's charge. Thus, dielectric friction is a charge-induced friction resulting from the finite relaxation time of the solvent dipoles surrounding the ion. The concept of dielectric friction was first introduced by Born in 1920, and was later developed by Fuoss [17], Boyd [18], Zwanzig [19], and Hubbard and Onsager [20,21]. Hubbard and Onsager have the most advanced *continuum* formulation of the dielectric friction model. In a simplified form, their expression for ion mobility is [14,20]

$$\mu_0 = \frac{q}{6\pi\eta r + \left(\frac{17}{280}\right) \cdot \frac{\tau q^2}{r^3 \epsilon}} \quad (2)$$

where  $\mu_0$  is the absolute mobility of the ion,  $q$  is the ion's charge,  $r$  is the radius of the ion, and  $\eta$ ,  $\epsilon$ , and  $\tau$  are the solvent viscosity, low-frequency dielectric constant, and dielectric relaxation time, respectively. The left-hand term in the denominator of Eq. (2) represents the hydrodynamic friction (Eq. (1)), and the right-hand term is the dielectric friction.

The Hubbard–Onsager model (Eq. (2)) is a continuum model in the sense that the ion is treated as an impenetrable sphere with a symmetric charge distribution, and the solvent is regarded as an incompressible fluid with a uniform viscosity, dielectric constant, and single dielectric relaxation time [20,22]. Further, the simplified Hubbard–Onsager equation (Eq. (2)) was derived for the case in which

hydrodynamic friction is dominant ( $\gg 50\%$  of the total friction) [21,22]. Without this simplifying condition, the friction coefficient in the denominator of Eq. (2) is expressed as an infinite series of higher order terms [21,22]. This simplifying condition is not obeyed by all of the analytes and solvent systems investigated herein; with the exception of the  $-1$  analytes in water and acetonitrile–water (30:70) media, dielectric friction is always greater than hydrodynamic friction. However, this does not affect the interpretation of the results. The goal of this paper is not to quantitatively predict the dielectric friction, but rather to use the Hubbard–Onsager model as guidance in explaining mobility trends. The Hubbard–Onsager model was successful at predicting solvent-induced selectivity changes in methanol–water [14] and acetonitrile (ACN)–water [15] media. However, it is questionable whether the Hubbard–Onsager model can be extended to solvent systems in which dielectric friction is much more pronounced. This paper investigates whether the *basic* solvent dependencies of Eq. (2) are maintained in these ‘new’ solvent systems.

These three factors ( $\text{pH}/\text{p}K_a$  effects, ionic strength effects, dielectric friction) act concurrently to alter ion selectivity in hydroorganic CE. In this paper, two of these factors, ionic strength effects and dielectric friction, are investigated as mechanisms for solvent-induced selectivity alterations in hydroorganic media containing ethanol and 2-propanol. Since these solvents have higher  $\tau/\varepsilon$  ratios than methanol and acetonitrile (see Eq. (2) and Table 1), it is expected that ions will experience greater dielectric friction in mixtures containing these solvents. The success of the Hubbard–Onsager dielectric friction model at predicting ion mobilities in ethanol–water and 2-

propanol–water media is evaluated. The success of the model at predicting the relative mobility trends between different solvents is also evaluated, revealing certain limitations of the Hubbard–Onsager model. Furthermore, the ionic strength behavior in ethanol–water and 2-propanol–water media are compared to those previously observed in methanol–water [14] and acetonitrile–water [15] media.

## 2. Experimental

### 2.1. Apparatus

All mobility measurements were performed on a P/ACE MDQ capillary electrophoresis system (Beckman Instruments, Fullerton, CA, USA), equipped with a UV absorbance detector set at 214 nm. A Pentium 300 MHz IBM computer using P/ACE Station Software for Windows 95 (Beckman Instruments) was used for data acquisition and control. The data acquisition rate was set at 4.0 Hz. The untreated fused-silica capillaries (Polymicro Technologies, Phoenix, AZ, USA) had inner diameters of 50  $\mu\text{m}$ , outer diameters of 365  $\mu\text{m}$ , and nominal total lengths of 60 cm (50 cm to detector). The precise lengths were determined after each set of experiments. New capillaries were conditioned by rinsing at high pressure (138 kPa) for 10 min with 1 *M* NaOH, 15 min with water, 5 min with 0.1 *M* NaOH, and finally for 10 min with water. Between runs, the capillaries were rinsed at high pressure for 3 min each with 0.1 *M* NaOH and water, respectively, followed by a 5 min rinse with the running buffer. Beakers containing aqueous–organic mixtures were placed in the instrument compartment to saturate the atmosphere, thereby eliminating evaporative losses from the solutions vials.

### 2.2. Chemicals

All solutions were prepared with Nanopure 18  $\text{M}\Omega$  water (Barnstead, Chicago, IL, USA). Buffers were prepared from reagent-grade sodium hydroxide (BDH, Darmstadt, Germany), reagent-grade sodium chloride (BDH), anhydrous ethanol (EtOH; Commercial Alcohols, Brampton, Canada), and ACS certified 2-propanol (2-PrOH; Fisher, Fair Lawn, NJ,

Table 1  
Properties of some common organic solvents [46]

Solvent	$\eta$ (cP)	$\varepsilon$	$\tau$ (ps)	$\tau/\varepsilon$ (ps)
Water	0.89	78.36	10	0.13
Methanol	0.55	32.66	53	1.62
Ethanol	1.08	24.55	143	5.82
2-Propanol	2.04	19.92	292	14.66
Acetonitrile	0.34	35.94	5	0.14
Formamide	3.30	111.0	108	0.97
Tetrahydrofuran	0.46	7.58	3	0.40
Dimethyl sulfoxide	1.99	46.45	21	0.45

USA). All solutions were filtered through 0.45  $\mu\text{m}$  Millex syringe-driven filters (Millipore, Bedford, MA, USA). All buffers consisted of 0.005  $M$  NaOH, prepared by dilution of a 0.1  $M$  stock solution, and the ionic strength was adjusted from 0.005 to 0.07  $M$  with the addition of NaCl. The required volume of organic solvent was added before final dilution with Nanopure water. The lower limit of ionic strength (0.005  $M$ ) was dictated by the concentration of sodium hydroxide required for sufficient buffering capacity. Sodium hydroxide can act as a buffer because strongly basic solutions show little change in pH when acid is added [23]. It was used in this study to ensure that all analytes were completely ionized, while avoiding the complicated task of measuring pH in mixed aqueous–organic solutions. Even though the  $pK_a$  of aromatic acids can increase by up to 2.5 units in the presence of some common alcohols [7–9], the sulfonates used in this study should still be completely ionized in the high pH NaOH solutions.

Chemicals for sample solutions were purchased from Aldrich (Milwaukee, WI, USA) and Eastman (Rochester, NY, USA). They were of reagent-grade or better, and used without any further purification. Sample anion solutions were prepared at concentrations of  $1 \times 10^{-3}$   $M$  in water, and were diluted to  $1 \times 10^{-4}$   $M$  in the corresponding buffer solution to eliminate sample stacking during electrophoresis. Mesityl oxide (Aldrich) was used as the neutral electroosmotic flow (EOF) marker.

### 2.3. Determination of absolute mobilities

With the addition of organic solvents to the buffers, the mobilities of the analytes became closely matched to that of the EOF, resulting in very long run times. This problem was overcome by using Williams and Vigh's method for mobility determination [24]. Briefly, a mixture of mesityl oxide and the analyte of interest was injected into the capillary for 4 s at 6.9–10.3 kPa, depending on the viscosity of the buffer. This sample plug was then transferred a certain distance into the capillary by applying a pressure of 10.3–17.2 kPa for 3–5 min. The analyte was then separated from mesityl oxide by applying a voltage for a variable amount of time, depending on the mobility of the analyte. For EtOH–water and

2-PrOH–water mixtures, the separation was performed at 10.0 kV for 4–6 min, and 9.0 kV for 5.5–9 min, respectively. Following this separation, mesityl oxide was injected into the capillary for 4 s at 6.9–10.3 kPa, and the three bands were pushed past the detector by applying a pressure of 10.3–17.2 kPa (again depending on solution viscosity). Effective mobilities were calculated as described elsewhere [14,24]. This method yields mobilities that are statistically equivalent at the 95% confidence level to those measured by the conventional method (results not shown). The field strengths are much less than  $10^4$  V/cm in this study. Therefore, the measured mobilities are independent of voltage (i.e. the *Wien effect* is not significant) [25].

Using the Pitts' equation [13], the absolute mobilities ( $\mu_o$ ) of the analytes were determined by plotting the effective mobilities against  $I^{1/2}/(1 + Ba \times I^{1/2})$ . Here,  $I$  is the buffer ionic strength and  $Ba$  is a constant that depends on the solvent composition (as described in the Results and discussion section). The effective mobilities were extrapolated to zero ionic strength by performing a linear least-squares regression, which yields the absolute mobility of the analyte,  $\mu_o$ .

### 2.4. Measurement of relative viscosity

The viscosities of the aqueous–organic buffers were measured relative to that of the pure aqueous buffer. For each of the buffers studied, mesityl oxide was injected into the capillary (4 s at 3.4 kPa), and was then pushed past the detector using 13.8 kPa pressure. The relative viscosities were determined from the ratios of the mesityl oxide elution times in the aqueous–organic and aqueous buffers.

## 3. Results and discussion

We have previously shown [14,15] that the Hubbard–Onsager theory of dielectric friction is useful in modeling selectivity changes on going from aqueous to mixed MeOH–water [14] or mixed ACN–water [15] media. It is therefore of interest to determine whether this model can be applied to other solvent systems in which dielectric friction effects are predicted to be more significant. Table 1 lists some

common organic solvents with their relevant properties. According to Eq. (2), dielectric friction becomes more significant with increasing  $\tau/\varepsilon$ . Therefore, out of the solvents listed in Table 1, ion mobility in hydroorganic media should be most strongly influenced by dielectric friction in the presence of EtOH and 2-PrOH. These solvents were thus chosen to study the applicability of the Hubbard–Onsager equation (Eq. (2)) to other solvent systems.

### 3.1. Ionic strength effects

The *absolute* mobility of an ion is independent of the buffer ionic strength. In the present study, the absolute mobilities of aromatic sulfonates ranging in charge from  $-1$  to  $-3$  were determined from the concentration-dependent *effective* mobilities using the Pitts' equation [13,14,25,26]

$$\mu_e \approx \mu_{e,o} - \left( \frac{41.25}{\eta(\varepsilon T)^{1/2} F} z_- + \frac{1.40 \cdot 10^6}{(\varepsilon T)^{3/2}} \times |z_+ z_-| \frac{2g}{1 + \sqrt{g}} \mu_{e,o} \right) \frac{\sqrt{I}}{1 + Ba\sqrt{I}} \quad (3)$$

where  $\mu_e$  is the effective mobility,  $\mu_{e,o}$  is the absolute mobility,  $z_-$  is the magnitude of the anion charge,  $z_+$  is the charge of the positive counterion,  $T$  is the temperature,  $F$  is the Faraday constant,  $a$  is an ion size parameter, and  $g$  is an electrolyte parameter equal to  $1/2$  for the 1:1 electrolyte studied herein.  $B$  is a constant defined by

$$B = \left( \frac{8\pi N_A e^2}{1000 \varepsilon k_B T} \right)^{1/2} \quad (4)$$

where  $N_A$  is Avogadro's number,  $e$  is the charge on an electron, and  $k_B$  is the Boltzmann constant. The left-hand term in the brackets of Eq. (3) is the *electrophoretic* effect, and the right-hand term in the brackets is the *relaxation* effect [13,14,27].

Li et al. [13] determined that the optimal value for  $Ba$  in Eq. (3) was 2.4 for a series of aromatic carboxylates, sulfonates, and phenols in aqueous media. For the ethanol–water and 2-propanol–water mixtures used herein, this constant was adjusted to reflect the change in dielectric constant as per Eq. (4), as described elsewhere [14,15]. Table 2 shows

Table 2  
Effect of buffer organic solvent content on solvent parameters, at 25 °C

Organic solvent (% v/v)	$\eta^a$ (cP)	$\varepsilon^c$	Approximated $\tau^e$
0	0.89 <sup>b</sup>	78.48 <sup>d</sup>	8.8 <sup>f</sup>
30 EtOH	1.96	64.39	44.7
60 EtOH	2.28	47.91	78.9
75 EtOH	2.00	39.08	100.9
30 2-PrOH	2.31	61.16	91.3
60 2-PrOH	3.03	40.49	161.0
75 2-PrOH	2.85	30.23	205.9

<sup>a</sup> Values calculated by multiplying the relative viscosity (see Experimental section) and the viscosity of water.

<sup>b</sup> Literature value [47].

<sup>c</sup> Values obtained from interpolation of literature data [48].

<sup>d</sup> Literature values [48].

<sup>e</sup> Approximated values of  $\tau$  calculated based on the assumption that the percentage difference between  $\tau$  (100% MeOH) and  $\tau$  ( $x\%$  MeOH) is the same as that between  $\tau$  (100% EtOH or 2-PrOH) and  $\tau$  ( $x\%$  EtOH or 2-PrOH).

<sup>f</sup> Literature value [14].

the viscosities and dielectric constants of the solvent mixtures used in this study. The adjusted  $Ba$  are 2.6, 3.1, and 3.4 for 30%, 60% and 75% EtOH, respectively, and 2.7, 3.3, and 3.9 for 30%, 60% and 75% 2-PrOH, respectively.

The results from the Pitts' plots, including the correlation coefficients, slopes, and intercepts (absolute mobilities,  $\mu_{e,o}$ ), are in Table 3. Some representative plots are shown in Fig. 1. Ion pairing effects were not a concern, since extrapolation to zero buffer ionic strength should correct for such effects. Furthermore, if ion association was significant, then curvature of the Pitts' plots would be expected. However, no significant curvature is evident in Fig. 1 or Table 3.

For all of the buffers studied herein, ions of higher charge experience greater ionic strength effects, as seen in Fig. 1 and Table 3. For any given buffer composition with the exception of 75% 2-PrOH, the Onsager slope of the  $-3$  sulfonate is always statistically larger than that of the  $-2$  sulfonate at the 95% confidence level. Similarly, except for 75% 2-PrOH, the Onsager slope of the  $-2$  sulfonate is always significantly larger than that of the  $-1$  sulfonate at the 95% confidence level. At 75% 2-PrOH, the Onsager slopes also increase with increasing analyte charge (Table 3), although the large uncertainty in

Table 3  
Ionic strength effects on organic anion mobilities in EtOH–water and 2-PrOH–water media<sup>a</sup>

Anion and solvent	Charge	Pitts equation		
		$R^2$	Onsager slope <sup>c</sup>	Intercept <sup>d</sup> , $\mu_0$
0% Organic solvent <sup>b</sup>				
Benzenesulfonate	–1	0.9847	–4.2±0.3	3.76±0.04
2,6-Naphthalenedisulfonate	–2	0.9905	–8.9±0.4	5.69±0.05
1,3,(6 or 7)-Naphthalenetrisulfonate	–3	0.9970	–14.4±0.4	7.55±0.05
30% EtOH				
Benzenesulfonate	–1	0.9974	–2.32±0.06	1.934±0.007
2,6-Naphthalenedisulfonate	–2	0.9984	–4.27±0.09	2.51±0.01
1,3,(6 or 7)-Naphthalenetrisulfonate	–3	0.9975	–7.0±0.2	3.24±0.02
60% EtOH				
Benzenesulfonate	–1	0.9949	–3.4±0.1	1.68±0.02
2,6-Naphthalenedisulfonate	–2	0.9991	–5.06±0.09	1.99±0.01
1,3,(6 or 7)-Naphthalenetrisulfonate	–3	0.9963	–6.7±0.3	2.18±0.04
75% EtOH				
Benzenesulfonate	–1	0.9987	–5.0±0.1	1.78±0.01
2,6-Naphthalenedisulfonate	–2	0.9976	–6.5±0.2	1.98±0.02
1,3,(6 or 7)-Naphthalenetrisulfonate	–3	0.9959	–8.3±0.3	2.03±0.03
30% 2-PrOH				
Benzenesulfonate	–1	0.9981	–2.02±0.05	1.658±0.006
2,6-Naphthalenedisulfonate	–2	0.9974	–3.7±0.1	2.09±0.01
1,3,(6 or 7)-Naphthalenetrisulfonate	–3	0.9960	–6.2±0.2	2.75±0.02
60% 2-PrOH				
Benzenesulfonate	–1	0.9963	–3.1±0.1	1.31±0.01
2,6-Naphthalenedisulfonate	–2	0.9990	–4.02±0.08	1.432±0.008
1,3,(6 or 7)-Naphthalenetrisulfonate	–3	0.9957	–5.7±0.2	1.56±0.03
75% 2-PrOH				
Benzenesulfonate	–1	0.9990	–4.42±0.08	1.241±0.008
2,6-Naphthalenedisulfonate	–2	0.9993	–4.77±0.07	1.210±0.008
1,3,(6 or 7)-Naphthalenetrisulfonate	–3	0.9973	–5.1±0.2	1.12±0.02

<sup>a</sup> Uncertainties are one standard deviation.

<sup>b</sup> From Ref. [14].

<sup>c</sup> Units =  $10^{-4} \text{ cm}^2 \text{ V}^{-1} \text{ s}^{-1} \text{ mol}^{-0.5} \text{ l}^{-0.5}$ .

<sup>d</sup> Units =  $10^{-4} \text{ cm}^2 \text{ V}^{-1} \text{ s}^{-1}$ .

the –3 slope does not allow for a statistical interpretation of the data. The trend of increasing ionic strength effect with increasing analyte charge is consistent with theory, since both terms in the brackets of Eq. (3) depend on the anion charge ( $z_-$ ). Similar behavior has been reported for aqueous [13], methanol–water [14], and acetonitrile–water [15] buffer systems. The charge-dependence of the ionic strength effect gives rise to the possibility of using

ionic strength to alter the selectivity between ions that differ in charge. Such selectivity changes have been frequently documented in the literature [28–30].

In the presence of organic solvents, the ionic strength-induced selectivity changes become more dramatic. For example, at 30% EtOH (Fig. 1a), the relative mobilities of the –1, –2 and –3 sulfonates are changed by varying the ionic strength, but the

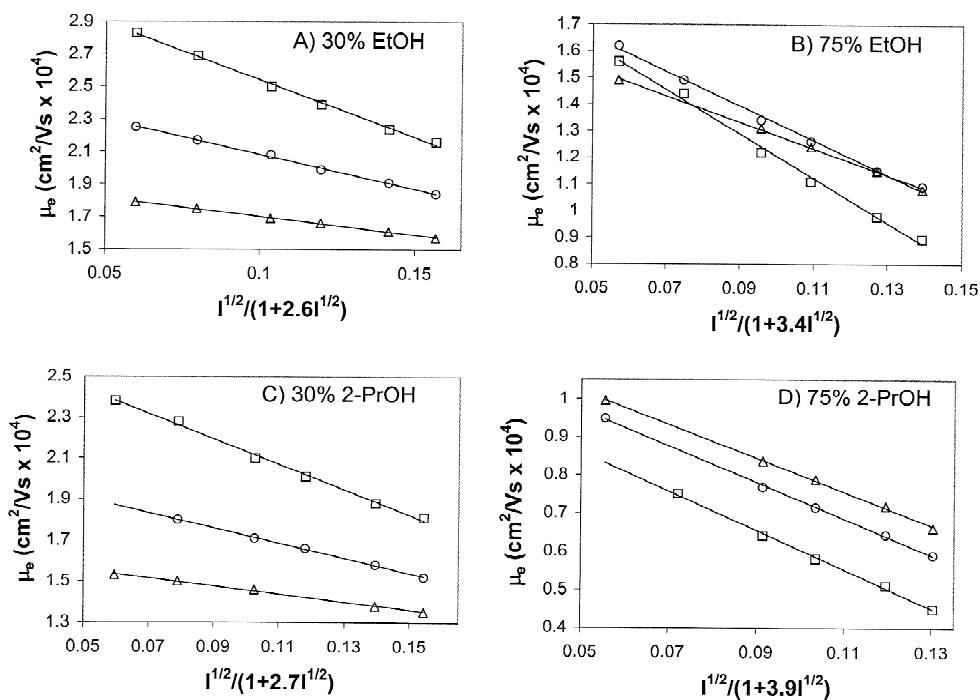


Fig. 1. Ionic strength effects on the mobilities of organic sulfonates for buffers containing (A) 30% EtOH, (B) 75% EtOH, (C) 30% 2-PrOH, and (D) 75% 2-PrOH. Solutes:  $\Delta$ , benzenesulfonate;  $\circ$ , 2,6-naphthalenedisulfonate;  $\square$ , 1,3,6 or 7-naphthalenetrisulfonate. Experimental conditions: UV detection at 214 nm; 60 cm capillary (50 cm to detector); 10 kV applied for (A)–(B), 9 kV applied for (C)–(D);  $1 \times 10^{-4}$  M sample concentration; 5 mM NaOH buffer, ionic strength adjusted using NaCl.

migration order remains the same (at least up to  $I=70$  mM). In contrast, at 75% EtOH (Fig. 1b), a migration order reversal is observed between the  $-1$  and  $-3$  sulfonates at  $I=20$  mM. The influence of the solvent composition and type on the ionic strength effect is discussed in the next section.

### 3.2. Influence of solvent composition and type on ionic strength effects

Using the data obtained herein (Fig. 1 and Table 3) and elsewhere [14,15], the effects of different compositions of MeOH–water, ACN–water, EtOH–water and 2-PrOH–water mixtures on the ionic strength effect are compared. Fig. 2 illustrates the variation in ionic strength effect (Onsager slope) with changes in the solvent composition and type for the  $-3$  sulfonate. For a buffer organic content of 30%, the Onsager slopes for all solvents are similar. In contrast, for the buffers containing 75% organic solvent, the Onsager slope for the acetonitrile mix-

ture is much larger than for all other solvents. This behavior can be explained based on the Pitts' equation (Eq. (3)). Previous studies in methanol–water [14] and acetonitrile–water [15] mixtures have shown that the electrophoretic effect (left-hand term in the brackets of Eq. (3)) is dominant. Thus, assuming that the electrophoretic effect is dominant, the Pitts' equation (Eq. (3)) can be expressed in a simplified form allowing only for the electrophoretic effect:

$$\mu \approx \mu_{\infty} - \left( \frac{41.25}{\eta(\epsilon T)^{1/2} F} z_- \right) \frac{\sqrt{I}}{1 + Ba\sqrt{I}} \quad (5)$$

The term in the brackets of Eq. (5) is the Onsager slope for the situation in which the electrophoretic effect is dominant. Therefore, it is expected that for different organic solvents, the relative magnitudes of the Onsager slopes (bracketed term in Eq. (5)) should vary as a function of  $z/(\eta\epsilon^{1/2})$ . That is, a plot of Onsager slope vs.  $z/(\eta\epsilon^{1/2})$  should give a straight line.

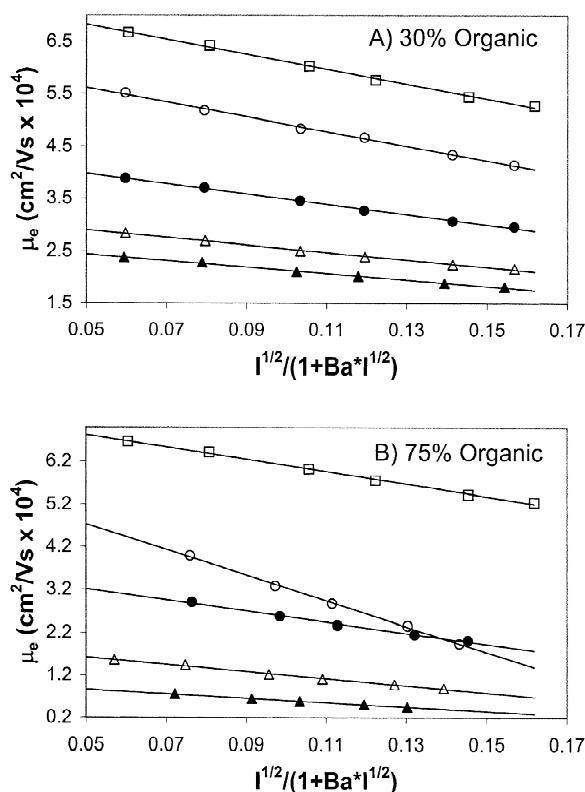


Fig. 2. Ionic strength effects on 1,3,6 or 7)-naphthalenetrisulfonate in media containing (A) 30% and (B) 75% organic solvent, as a function of organic modifier. The data for purely aqueous media, 30% MeOH, and 75% MeOH is from Ref. [14]. The data for 30% ACN and 75% ACN is from Ref. [15]. Organic modifiers:  $\square$ , purely aqueous media;  $\circ$ , ACN;  $\bullet$ , MeOH;  $\triangle$ , EtOH;  $\blacktriangle$ , 2-PrOH. Experimental conditions as reported in Fig. 1 and elsewhere [14,15].

Fig. 3 is a plot of Onsager slope vs.  $z/(\eta\epsilon^{1/2})$  for the three sulfonates under investigation, constructed using the data for pure water [14] and for aqueous mixtures of 30, 60 and 75% methanol [14], acetonitrile [15], ethanol and 2-propanol. As predicted by Eq. (5), this plot shows good correlation, with a linear correlation coefficient,  $R^2$ , of 0.95. Therefore, upon changing the organic solvent content and type, the Onsager slope for a given ion will change as a function of the solvent parameter  $1/(\eta\epsilon^{1/2})$ . This explains the trends in Onsager slopes seen herein (Fig. 2 and Table 3) and in Refs. [14,15]. For example, the large slope observed for the  $-3$  sulfonate in 75% ACN (Fig. 2b) can be attributed to

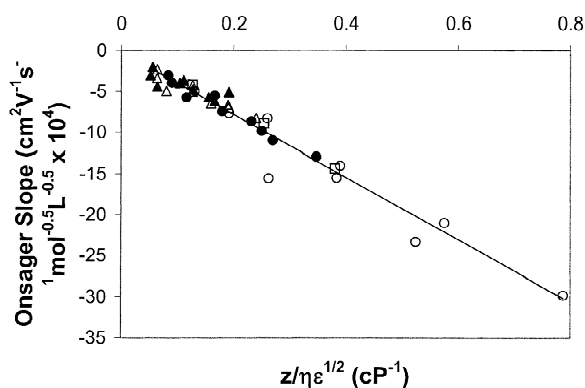


Fig. 3. Correlation plot showing the influence of solvent composition and type on the ionic strength effects for the  $-1$ ,  $-2$  and  $-3$  sulfonates. The plot was constructed using the data for pure water and for aqueous mixtures of 30%, 60%, and 75% methanol, acetonitrile, ethanol, and 2-propanol. The data for pure water and MeOH–water mixtures are from Ref. [14]. The data for ACN–water mixtures is from Ref. [15]. Organic modifiers:  $\square$ , purely aqueous media;  $\circ$ , ACN;  $\bullet$ , MeOH;  $\triangle$ , EtOH;  $\blacktriangle$ , 2-PrOH.

the low viscosity of this solvent mixture [15], which leads to a large value of  $1/(\eta\epsilon^{1/2})$  and consequently to a large Onsager slope. Indeed, the parameter  $1/(\eta\epsilon^{1/2})$  in 75% ACN is 3.3 times greater than that in 75% EtOH, which is consistent with the 3.6-fold increase in Onsager slope between 75% EtOH and 75% ACN. At an organic content of 30%, the solvent parameter  $1/(\eta\epsilon^{1/2})$  does not vary as dramatically between solvents, which accounts for the similar slopes observed in Fig. 2a. Nonetheless,  $1/(\eta\epsilon^{1/2})$  still increases by a factor of 2.1 between 30% ACN and 30% EtOH, which is consistent with the 2.0-fold increase in slope observed in Fig. 2a.

In general, for the slopes that are significantly different at the 95% confidence level, the following order is always observed at any given organic solvent content: Onsager slope in ACN > MeOH > EtOH > 2-PrOH. This is in agreement with the relative sizes of the parameter  $1/(\eta\epsilon^{1/2})$  predicted by the data in Table 1.

### 3.3. Dielectric friction

According to the Hückel equation (Eq. (1)), the Walden product ( $\mu_o\eta$ ) should be a constant for a given ion, regardless of the solvent composition. A plot of  $\mu_o\eta$  vs. solvent composition should then be



horizontal if hydrodynamic friction is the only friction experienced by the ion. However, in previous studies involving methanol–water [14] and acetonitrile–water [15] media, a negative deviation was observed in plots of the Walden product versus increasing organic solvent content. This was due to the increase in dielectric friction with increasing organic modifier concentration. Furthermore, dielectric friction effects were more dramatic for ions of higher charge-to-size. In the present studies involving ethanol–water and 2-propanol–water media, the Walden products were plotted against % organic modifier to investigate the influence of dielectric friction on mobility. The corresponding plots are in Fig. 4. Since all anions studied herein are similar in size, further discussions will refer to the ‘charge’ dependence, rather than the ‘ $q^2/r^3$ ’ dependence, of dielectric friction.

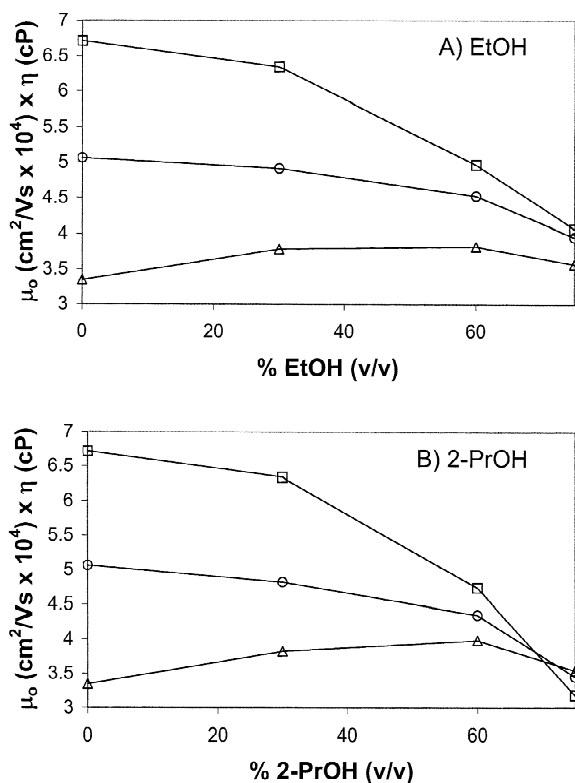


Fig. 4. Dependence of Walden product on the organic content of the buffer for (A) EtOH and (B) 2-PrOH. Legend and experimental conditions as in Fig. 1. The data for 0% EtOH and 0% 2-PrOH are from Ref. [14].

The dielectric constant decreases as the ethanol or 2-propanol content increases (Table 2). Unfortunately, dielectric relaxation times for these mixed solvents are not available in the literature. However, it is assumed that  $\tau$  increases with ethanol or 2-propanol content in a similar manner as in methanol–water mixtures [14]. Table 2 lists approximated values of  $\tau$  for the EtOH–water and 2-PrOH–water solutions. Therefore, according to the Hubbard–Onsager equation (Eq. (2)) and Table 2, dielectric friction should increase with increasing EtOH or 2-PrOH content.

In Fig. 4, the negative deviation from the ideal Hückel (horizontal) behavior for the  $-2$  and  $-3$  sulfonates increases with increasing EtOH and 2-PrOH content. This is consistent with the increase in dielectric friction predicted by the Hubbard–Onsager equation (Eq. (2)). Also seen in Fig. 4 is a more dramatic deviation from ideal Hückel behavior with increasing analyte charge. This is consistent with the charge dependence of the dielectric friction term in the Hubbard–Onsager equation (right-hand term in the denominator of Eq. (2)). As a result, changes in the relative mobilities of ions differing in charge are observed. The relative absolute mobilities of the  $-1$ ,  $-2$  and  $-3$  sulfonates are altered on going from 0% to 75% EtOH, but the migration order is not changed. In contrast, a complete reversal in migration order is observed at 75% 2-PrOH, whereby the migration order is:  $\mu_{o,-1} > \mu_{o,-2} > \mu_{o,-3}$ . Therefore, in both EtOH–water and 2-PrOH–water media, dielectric friction can cause selectivity alterations between analytes that differ in charge. The more dramatic selectivity changes observed with 2-PrOH–water are expected based on the greater dielectric friction predicted for 2-PrOH–water media than for EtOH–water media (Eq. (2), Table 2). The influence of solvent type on dielectric friction is discussed in Section 3.4.

As seen in Fig. 4, a positive deviation from ideal Hückel (horizontal) behavior is observed for the  $-1$  sulfonate in EtOH–water and 2-PrOH–water media. This suggests that this ion is experiencing *less* friction than that predicted solely by the Hückel equation. Similar behavior has been previously reported. In ethanol–water [8] and propanol–water [9] media, Sarmini and Kennedler observed that the product of *effective* mobility and viscosity for non-

hydroxy-substituted singly-charged aromatic acids increased slightly with increasing organic content. Similarly, Steel et al. [31] showed that in the presence of sucrose, mannitol or glycerol, the conductivity of small ions like  $H^+$  follow the relation  $\lambda_i^0 \eta^x = \text{constant}$ , where  $x < 1$  [32]. Further, Ibuki and Nakahara [33–36] reported negative residual friction coefficients (total friction minus Stokes' friction) for alkylammonium ions and large halide ions in aqueous media and in media consisting of various amounts of methanol, ethanol, and 1-propanol. A possible mechanism, the “passing-through-cavities” mechanism, has been proposed to explain this anomalous increase in mobility [37–40].

### 3.4. Influence of solvent type on dielectric friction

According to the Hubbard–Onsager equation (Eq. (2)), solvents with higher relaxation times ( $\tau$ ) and lower dielectric constants ( $\epsilon$ ) should experience greater dielectric friction effects. Therefore, from the data presented herein (Tables 1 and 2) and elsewhere [14,15], it is expected that hydro-organic media containing acetonitrile, methanol, ethanol, or 2-propanol will experience increasing amounts of dielectric friction, respectively. Fig. 5 plots the Walden product ( $\mu_o \eta$ ) for the  $-3$  sulfonate as a function of

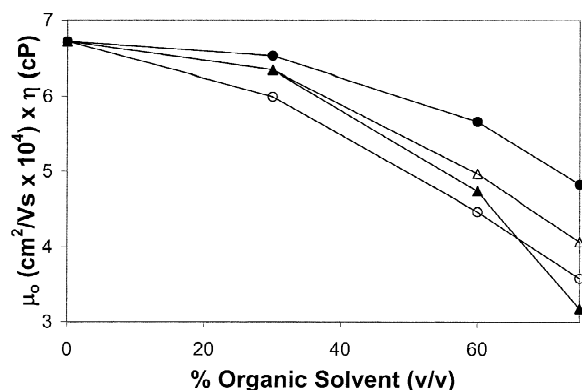


Fig. 5. Influence of solvent type on the dielectric friction experienced by 1,3,6 or 7-naphthalenetrisulfonate. ○, ACN; ●, MeOH; △, EtOH; ▲, 2-PrOH. The data for pure water and methanol are from Ref. [14]. The data for acetonitrile is from Ref. [15].

organic solvent content and type. The larger the dielectric friction effects, the more significant is the negative deviation from ideal Hückel (horizontal) behavior.

As seen in Fig. 5, the observed trend for the alcohols is that the dielectric friction in 2-PrOH–water > EtOH–water > MeOH–water. This is consistent with the trend predicted from the Hubbard–Onsager equation (Eq. (2)). Further, upon changing alcohol type, the relative changes in dielectric friction observed in Fig. 5 are consistent with theory. This can be seen by rearranging the Hubbard–Onsager equation (Eq. (2)) into the following form

$$\frac{1}{\mu_o \eta} = \frac{6\pi r}{q} + \left(\frac{17}{280}\right) \cdot \frac{\tau q}{r^3 \eta \epsilon} \quad (6)$$

Accordingly, for a given ion, individual plots of  $1/\mu_o \eta$  vs.  $\tau/\eta \epsilon$  constructed for each solvent type should all possess the same slope and intercept. Such plots were constructed for the  $-3$  sulfonate in MeOH–water, EtOH–water and 2-PrOH–water media using the data presented in Table 2 and in Ref. [14]. Although only *approximated* values of  $\tau$  were used for the EtOH–water and 2-PrOH–water mixtures (Table 2), the resulting plots for these solvent mixtures had slopes and intercepts that were not significantly different at the 95% confidence level from those obtained in MeOH–water (results not shown). Therefore, within a given class of organic solvents (i.e. alcohols), the Hubbard–Onsager model is successful at predicting the relative inter-solvent mobility trends in mixed aqueous–organic media.

We have previously demonstrated that for hydro-organic media containing MeOH [14] or ACN [15], the magnitude of the negative deviation from ideal Hückel behavior for each of these solvents was consistent with the Hubbard–Onsager model. This was evident by a strong linear correlation between  $1/\mu_o \eta$  and  $\tau/\eta \epsilon$  for these solvents. However, according to the Hubbard–Onsager equation (Eq. (2)) and the data in Table 1, ions in ACN–water media are expected to experience less dielectric friction than in MeOH–water media. This is contrary to what is observed in Fig. 5, where the  $-3$  sulfonate experiences more dielectric friction in 30% and 60% ACN than in 30% and 60% 2-PrOH! Further, at 75%

ACN, the  $-3$  sulfonate is affected more by dielectric friction than in 75% EtOH. Therefore, it appears as though the  $-3$  sulfonate is experiencing proportionally more dielectric friction in ACN–water than would be predicted based on the observed behavior of the alcohols. As mentioned above, plots of  $1/\mu_o\eta$  vs.  $\tau/\varepsilon\eta$  for the ACN–water and MeOH–water solvent systems should have the same slopes and intercepts. However, at the 95% confidence level, the slope and intercept for the ACN–water media were statistically larger and smaller, respectively, than those for the MeOH–water media. This apparent failure of the Hubbard–Onsager model may result from the continuum nature of the model. As a continuum dielectric friction model, the Hubbard–Onsager theory does not allow for the microscopic nature of ion motion in terms of the solvent structure or the ion–solvent interactions [41,42]. In other words, it considers only the bulk properties of the solvent ( $\eta$ ,  $\varepsilon$ ,  $\tau$ ) and does not differentiate between solvents with different microscopic properties (i.e. ion–solvent interactions).

The alcohols studied herein (methanol, ethanol, 2-propanol) and acetonitrile belong to two distinct classes of solvents. The alcohols are *protic* solvents, meaning that these solvents are hydrogen-bonded [43]. On the other hand, acetonitrile is *aprotic* and *dipolar* because it is a non-hydrogen-bonded solvent that has a high dielectric constant [43]. These two classes of solvents exhibit very different ion–solvent interactions. In protic solvents, hydrogen bonding and ion–dipole interactions are important, whereas in dipolar aprotic solvents, both ion–dipole interactions and interactions due to the mutual polarizability of the ion and solvent are important [44]. Since the Hubbard–Onsager dielectric friction model does not consider these differences in ion–solvent interactions, it will likely not predict the relative behavior of ions among these different classes of organic solvents. This is indeed the case in Fig. 5, where the  $-3$  sulfonate experiences proportionally more dielectric friction in ACN–water media than in alcohol–water media, which is contrary to what is expected based on the Hubbard–Onsager equation (Eq. (2)). However, within a given class of solvents (i.e. alcohol–water mixtures) in which the ion–solvent interactions are the same, the Hubbard–Onsager

model successfully describes the relative behavior of ions in mixed aqueous–organic media. A molecular model, which takes into account solvent structure and ion–solvent interactions, would undoubtedly be more successful at predicting the relative mobility trends observed between different classes of solvents.

Hosoi and Masuda [45] have also observed that the frictional coefficients experienced by the perchlorate ion in alcohols are less than those predicted by the Hubbard–Onsager electrohydrodynamic model when the classical Debye dielectric relaxation times (as used herein) are used for the calculations. In contrast, they found good agreement between the observed and calculated frictional coefficients in other solvents, including acetonitrile. The smaller-than-expected friction in alcohol is consistent with the results presented herein (Fig. 5), in which the  $-3$  sulfonate experienced less dielectric friction in media containing alcohol than in media containing acetonitrile. Hosoi and Masuda explained that the anomalous behavior of the alcohols resulted from the shorter time scale of the translational motion of the perchlorate ion compared to the relaxation times of the alcohols [45]. As a result, the perchlorate ion did not feel the full dielectric friction predicted by the long relaxation times of the alcohols. Under these conditions, the contribution of local ion–solvent interactions to the overall ion motion becomes important [45]. Clearly, a molecular model would be more successful than a continuum model at predicting the behavior of ions in hydroorganic media containing alcohol.

It is important to note that the negative deviations from ideal Hückel behavior for both ACN–water and MeOH–water media are consistent with the dielectric friction model of Hubbard and Onsager. This is evident from the good linear correlation between  $1/\mu_o\eta$  and  $\tau/\varepsilon\eta$  for these solvent systems [14,15]. Therefore, the inability of the Hubbard–Onsager model at predicting the relative behavior of ions between different classes of solvents does not imply that the model is effective for one class of solvent (i.e. acetonitrile) and ineffective for another (i.e. alcohols). It simply reflects the fact that the model is limited by its continuum nature. For a given solvent type, the Hubbard–Onsager dielectric friction model

remains a useful tool for explaining the selectivity changes that are observed upon going from aqueous to mixed aqueous–organic media.

#### 4. Conclusions

Regardless of whether the electrophoretic media is purely aqueous or contains ethanol or 2-propanol, ions of higher charge experience larger ionic strength effects. Therefore, for all solvents investigated herein, varying the buffer ionic strength can cause significant selectivity changes between ions that differ in charge. Furthermore, these ionic-strength induced selectivity alterations are more dramatic when organic solvents are present in the media. For different organic modifier types and contents, the ionic strength effect is governed to a large extent by the electrophoretic effect of the Pitts equation (left-hand term in the brackets of Eq. (3)). As such, the ionic strength effect increases with increasing solvent  $1/(\eta\varepsilon^{1/2})$ .

The Hubbard–Onsager theory of dielectric friction is successful at predicting the behavior of  $-2$  and  $-3$  sulfonates in media containing ethanol and 2-propanol. As predicted by the Hubbard–Onsager equation (Eq. (2)), an increase in dielectric friction is observed with increasing organic content and with increasing analyte charge. This results in solvent-induced changes in the relative mobilities of ions differing in charge. Further, within a given class of solvents (alcohol–water mixtures), the Hubbard–Onsager model is successful at predicting the *relative* mobility trends observed between MeOH–water, EtOH–water and 2-PrOH–water media. However, when compared with the alcohol–water media, the relative ion mobilities observed for ACN–water media are not consistent with the Hubbard–Onsager equation. This apparent failure may be explained by the continuum nature of the model, whereby ion–solvent interactions are not taken into account. Since different solvent classes possess different ion–solvent interactions, a continuum dielectric friction model will likely not correctly predict the relative behavior of ions between different classes of solvents. Nonetheless, for a given solvent type, the dielectric friction model of Hubbard and Onsager

remains a useful tool in predicting solvent-dependent selectivity changes.

#### Acknowledgements

This work was supported by the Natural Sciences and Engineering Research Council of Canada (NSERC), and the University of Alberta. K.I.R. gratefully acknowledges her NSERC Postgraduate Scholarship.

#### References

- [1] P.B. Wright, A.S. Lister, J.G. Dorsey, *Anal. Chem.* 69 (1997) 3251.
- [2] A. Karbaum, T. Jira, *Electrophoresis* 20 (1999) 3396.
- [3] A. Jouyban-Gharamaleki, M.G. Khaledi, B.J. Clark, *J. Chromatogr. A* 868 (2000) 277.
- [4] C.A. Lucy, *J. Chromatogr. A* 850 (1999) 319.
- [5] K. Sarmini, E. Kenndler, *J. Chromatogr. A* 833 (1999) 245.
- [6] K. Sarmini, E. Kenndler, *J. Cap. Elec.* 5 (1998) 103.
- [7] K. Sarmini, E. Kenndler, *J. Chromatogr. A* 806 (1998) 325.
- [8] K. Sarmini, E. Kenndler, *J. Chromatogr. A* 811 (1998) 201.
- [9] K. Sarmini, E. Kenndler, *J. Chromatogr. A* 818 (1998) 209.
- [10] Y.C. Guillaume, E. Peyrin, A. Ravel, C. Guinchard, *J. Liq. Chromatogr. Rel. Technol.* 23 (2000) 2789.
- [11] D. Barrón, A. Irlés, J. Barbosa, *J. Chromatogr. A* 871 (2000) 367.
- [12] D. Barrón, E. Jiménez-Lozano, A. Irlés, J. Barbosa, *J. Chromatogr. A* 871 (2000) 381.
- [13] D.M. Li, S.L. Fu, C.A. Lucy, *Anal. Chem.* 71 (1999) 687.
- [14] K.I. Roy, C.A. Lucy, *Anal. Chem.* 73 (2001) 3854.
- [15] K.I. Roy, C.A. Lucy, *Electrophoresis* 23 (2002) 383.
- [16] P. Colonomos, P.G. Wolynes, *J. Chem. Phys.* 71 (1979) 2644.
- [17] R.M. Fuoss, *Proc. Natl. Acad. Sci.* 45 (1959) 807.
- [18] R.H. Boyd, *J. Chem. Phys.* 35 (1961) 1281.
- [19] R. Zwanzig, *J. Chem. Phys.* 38 (1963) 1603.
- [20] J. Hubbard, L. Onsager, *J. Chem. Phys.* 67 (1977) 4850.
- [21] J.B. Hubbard, *J. Chem. Phys.* 68 (1978) 1649.
- [22] D.F. Evans, T. Tominaga, J.B. Hubbard, P.G. Wolynes, *J. Phys. Chem.* 83 (1979) 2669.
- [23] D.D. Perrin, B. Dempsey, *Buffers for pH and Metal Ion Control*, Chapman and Hall, London, 1974.
- [24] B.A. Williams, G. Vigh, *Anal. Chem.* 68 (1996) 1174.
- [25] T. Erdey-Grúz, *Transport Phenomena in Aqueous Solutions*, Wiley, New York, 1974, Ch. 4.
- [26] H. Falkenhagen, G. Kelbg, in: J.O.M. Bockris (Ed.), *Modern Aspects of Electrochemistry*, Vol. 2, Butterworths, London, 1959, pp. 1–86, Ch. 1, eq 235.
- [27] J.O.M. Bockris, A.K.N. Reddy, *Modern Electrochemistry*, Vol. 1, Plenum Press, New York, 1970, pp. 420–440.

- [28] W. Friedl, J.C. Reijenga, E. Kenndler, *J. Chromatogr. A* 709 (1995) 163.
- [29] Y. Mechref, G.K. Ostrander, Z. El Rassi, *J. Chromatogr. A* 792 (1997) 75.
- [30] M.I.T. Carou, P.L. Mahía, S.M. Lorenzo, E.F. Fernández, D.P. Rodríguez, *J. Chromatogr. A* 918 (2001) 411.
- [31] B.J. Steel, J.M. Stokes, R.H. Stokes, *J. Phys. Chem.* 62 (1958) 1514.
- [32] H. Sadek, *J. Electroanal. Chem.* 144 (1983) 11.
- [33] K. Ibuki, M. Nakahara, *J. Chem. Phys.* 84 (1986) 2776.
- [34] K. Ibuki, M. Nakahara, *J. Phys. Chem.* 90 (1986) 6362.
- [35] K. Ibuki, M. Nakahara, *J. Phys. Chem.* 91 (1987) 1864.
- [36] K. Ibuki, M. Nakahara, *J. Phys. Chem.* 91 (1987) 4411.
- [37] N. Takisawa, J. Osugi, M. Nakahara, *J. Phys. Chem.* 85 (1981) 3582.
- [38] N. Takisawa, J. Osugi, M. Nakahara, *J. Chem. Phys.* 77 (1982) 4717.
- [39] N. Takisawa, J. Osugi, M. Nakahara, *J. Chem. Phys.* 78 (1983) 2591.
- [40] M. Nakahara, T. Török, N. Takisawa, J. Osugi, *J. Chem. Phys.* 76 (1982) 5145.
- [41] R. Biswas, B. Bagchi, *J. Chem. Phys.* 106 (1997) 5587.
- [42] P.G. Wolynes, *J. Chem. Phys.* 68 (1978) 473.
- [43] E.J. King, in: A.K. Covington, T. Dickinson (Eds.), *Physical Chemistry of Organic Solvent Systems*, Plenum Press, New York, 1973, pp. 331–393.
- [44] E. Price, in: J.J. Lagowski (Ed.), *The Chemistry of Non-Aqueous Solvents*, Vol. 1, Academic Press, New York, 1966, pp. 67–96.
- [45] H. Hosoi, Y. Masuda, *J. Phys. Chem. B* 102 (1998) 2995.
- [46] H.D.B. Jenkins, Y. Marcus, *Chem. Rev.* 95 (1995) 2695.
- [47] *CRC Handbook of Chemistry and Physics*, 76th ed, CRC Press, New York, 1995–1996.
- [48] Y.Y. Akhadov, *Dielectric Properties of Binary Solutions—A Data Handbook*, Pergamon Press, New York, 1980.